Aerosol Science and Technology

ISSN: 0278-6826 (Print) 1521-7388 (Online) Journal homepage: http://www.tandfonline.com/loi/uast20

Physical and Chemical Characteristics and Volatility of PM in the Proximity of a Light-Duty Vehicle Freeway

Thomas Kuhn , Subhasis Biswas , Philip M. Fine , Michael Geller & Constantinos Sioutas

To cite this article: Thomas Kuhn , Subhasis Biswas , Philip M. Fine , Michael Geller & Constantinos Sioutas (2005) Physical and Chemical Characteristics and Volatility of PM in the Proximity of a Light-Duty Vehicle Freeway, Aerosol Science and Technology, 39:4, 347-357, DOI: 10.1080/027868290930024

To link to this article: http://dx.doi.org/10.1080/027868290930024

Published online: 23 Feb 2007.

Submit your article to this journal

Article views: 374

View related articles

Citing articles: 25 View citing articles

Full Terms & Conditions of access and use can be found at
http://www.tandfonline.com/action/journalInformation?journalCode=uast20

Download by: [University of North Texas] **Date:** 06 January 2017, At: 21:54

Aerosol Science and Technology, 39:347–357, 2005
Copyright © American Association for Aerosol Research
ISSN: 0278-6826 print / 1521-7388 online
DOI: 10.1080/027868290930024

Physical and Chemical Characteristics and Volatility of PM in the Proximity of a Light-Duty Vehicle Freeway

Thomas Kuhn,[1] Subhasis Biswas,[2] Philip M. Fine,[2] Michael Geller,[2] and Constantinos Sioutas[2]

[1]*Southern California Particle Center and Supersite, Institute of the Environment, University of California, Los Angeles, California*
[2]*Department of Civil and Environmental Engineering, University of Southern California, Los Angeles, California*

Volatility properties of ultrafine particles were analyzed next to State Route 110 (Pasadena freeway CA), a light-duty vehicle freeway where heavy-duty traffic is prohibited. In addition, mass concentration and chemical composition of particulate matter (PM) were measured in coarse, accumulation, and ultrafine modes. On weekdays from 17 May to 4 June 2004, measurements were performed in two locations, one very close to the freeway (within 2.5 m from the curb) and one at a distance of about 50 m from the freeway. For measurement of mass and chemical composition, the study employed in each location a micro-orifice uniform deposit impactor (MOUDI) and a modified high-volume sampler. Both instruments sampled with the same size cutpoints: a coarse mode from 2.5 to 10 μm, an accumulation mode from 0.18 to 2.5 μm, and an ultrafine mode of particles less than 0.18 μm in aerodynamic diameter. Alternately, a tandem differential mobility analyzer (TDMA) was used at the two sites. A heater between the two DMAs evaporated volatile material from the monodisperse aerosol, size selected by the first DMA. The second DMA analyzed the losses of volatile components. The ultrafine number concentrations next to the freeway were 46,000 cm^{-3} on average during the sampling period. The MOUDI ultrafine mass concentration, nitrate, and EC were higher next to the freeway than at the background site farther from the freeway. The other components analyzed in the ultrafine mode had similar concentrations next to the freeway and at the background site. Volatility ranged from about 65% volume losses of 120 nm particles heated to 110°C to 95% of 20 nm particles. The 20 nm aerosol was only internally mixed, whereas increasing nonvolatile fractions were found for 40 nm (6% next to the freeway), 80 nm (20%), and 120 nm (28%) aerosols.

Received 23 September 2004; accepted 27 January 2005.

The authors would like to express their sincere gratitude to all of the study participants for their cooperation during data collection and analysis, in particular to Bhabesh Chakrabarti and Harish Phuleria. Special thanks to the City of Los Angeles Department of Recreation and Parks for allowing us the use of the Arroyo Seco Park. This work was supported by the Southern California Particle Center and Supersite: US Environmental Protection Agency grant number R82735201, California Air Resources Board contract number 98-316.

Address correspondence to Thomas Kuhn, Department of Civil and Environmental Engineering, University of Southern California, Los Angeles, CA 90089, USA. E-mail: tkuhn@usc.edu

INTRODUCTION

Epidemiological and toxicological studies have demonstrated strong links between ambient particulate matter mass exposure and adverse health outcomes (National Research Council 2004). However, it is not clear which physical or chemical properties of particulate matter (PM) pose the greatest health risk. Recent results have shown that ultrafine particles are more toxic than larger particles (Donaldson et al. 2002; Li et al. 2003; Oberdörster 2000; Pietropaoli et al. 2004). Furthermore, individual particles have been shown to be capable of inducing mitochondrial damage (Li et al. 2003), suggesting that particle number concentrations, which are dominated by ultrafine particles, may be more indicative of some potential health impacts than particle mass concentrations. In urban environments the dominant sources of ultrafine particles are direct emissions from motor vehicles and secondary PM formed by photochemical or physical processes in the atmosphere (Fine et al. 2004b; Zhang et al. 2004b).

Measurements of particle emissions from motor vehicles have been accomplished via dynamometer source testing (Chase et al. 2000; Kwon et al. 2003; Sakurai et al. 2003a, 2003b; Schauer et al. 1999, 2002; Suess and Prather 2002), roadway tunnel sampling (Allen et al. 2001; Fraser et al. 1998; Laschober et al. 2004; McGaughey et al. 2004), on-road chase experiments (Shah et al. 2004; Vogt et al. 2003), and roadside measurements (Harrison et al. 2003; Sturm et al. 2003; Zhu et al. 2002a, 2002b, 2004). In general, particles directly emitted from motor vehicles are in the size range from 20 to 130 nm in aerodynamic diameter for diesel engines (Morawska et al. 1998) and from 20 to 60 nm for gasoline engines (Ristovski et al. 1998). It is known that many of the organic chemical constituents of PM emitted from vehicles are semivolatile, existing simultaneously in the gas and particle phases at equilibrium (Schauer et al. 1999, 2002). Thus, changes in ambient temperature and gas-phase

concentrations of these components can affect the measured particle size distributions due to evaporation or condensation. For this reason, it has been shown that the particle size distributions determined by dynamometer testing are dependent on the dilution ratios and dilution air conditions of the sampling apparatus (Holmen and Qu 2004; Lyyranen et al. 2004; Vaaraslahti et al. 2002). Road tunnel sampling is also subject to the unusual dilution and temperature conditions found in the tunnel.

Roadside measurements, as opposed to chase studies, offer the opportunity to measure particle size distributions averaged over the emissions from thousands of vehicles under "real-world" conditions (Hitchins et al. 2000). Zhu et al. (2002b) measured the size distributions of PM and the concentrations of gaseous copollutants in the proximity of a freeway mostly impacted by gasoline vehicles in West Los Angeles. Particle number concentrations (in the range from 6 to 220 nm) decreased more quickly with downwind distance from the freeway than CO and black carbon. Zhu et al. (2002a) obtained similar data in the vicinity of a freeway impacted heavily by heavy-duty diesel traffic. When these experiments were repeated in winter with cooler ambient temperatures and less atmospheric mixing (Zhu et al. 2004), particle number concentrations in the smallest size ranges were significantly higher.

Zhang et al. (2004b) demonstrated that condensation, evaporation, and dilution were the major factors affecting aerosol size distributions in the first 250 m downwind from freeways. The high concentrations of particle numbers in the proximity of freeways raises concerns for population exposure during commute. The particle volatility, which causes the dynamically shifting size distributions of these freshly emitted particles, needs to be better characterized to assess accurately population exposure to the physical and chemical properties of PM.

A few previous studies have measured the volatility of PM in dynamometer tests using tandem differential mobility analyzer (TDMA) systems (e.g., Sakurai et al. 2003a). However, given the dependence of dynamometer tests on dilution conditions, assessment of the volatility of vehicular PM emissions under real-world conditions is needed. A previous roadside study measured the volatility of ultrafine PM downwind of a mixed heavy- and light-duty traffic freeway at two different distances both indoors and outdoors (Kuhn et al. 2005). The current study measured PM volatility properties next to a pure gasoline freeway where heavy-duty diesel vehicles are prohibited. Additional measurements were made of coarse, accumulation, and ultrafine PM mode mass and chemistry. Results will help to determine the properties of particles to which people are exposed in the vicinity of freeways.

METHODS

Sampling Location and Schedule

Measurements were conducted at the State Route 110 (SR 110), between downtown Los Angeles and Pasadena, CA (USA), where the freeway runs generally north–south. On this stretch of the freeway—Historic Arroyo Seco Parkway, the first freeway in the Western U.S.—only light-duty vehicles are allowed. This offers the unique opportunity of studying emissions from light-duty traffic under ambient conditions. The relatively short stretch of freeway offered a limited choice of sampling sites and, after evaluating the possibilities, Hermon Park in the Arroyo Seco on the east side, directly adjacent to the freeway (Figure **??**) was chosen. This site was selected mainly for easy access to the freeway and available space close to the freeway not directly influenced by local street traffic. At Hermon Park, the freeway runs in southwest–northeast direction and has three north- and three southbound lanes, a crash barrier in the center, and no emergency lanes. The park is at the same level as the freeway, only slightly raised by less than 0.5 m.

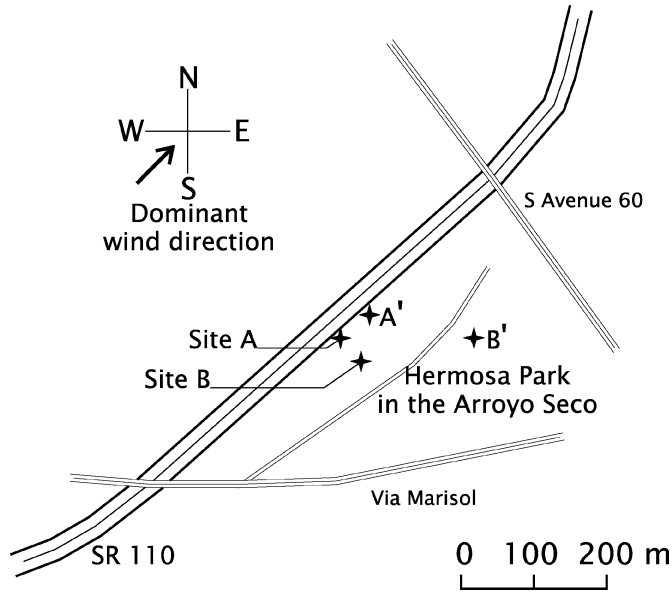

FIG. 1. Sampling sites at SR 110.

The study took place from 17 May to 4 June 2004. Sampling was conducted on weekdays from about 12 pm to 7 pm, which captured the evening rush-hour traffic. This sampling period represented typical summertime conditions in Los Angeles. The meteorological conditions are expected to influence particle volatility properties, as conditions for condensation of fresh ultrafine particles and evaporation of volatile material from these particles depend, among other parameters, on ambient temperature and humidity. It is therefore planned to repeat this study in the winter season so that seasonal variability can be addressed as well.

Measurements of particle volatility were carried out at two different locations. One was next to the edge of the northbound lanes of SR 110 (Site A: see Figure **??**). The aerosol at this sampling site is heavily influenced by the freeway traffic. The sampling inlet was approximately 2.5 m away from the curb of the freeway. Site A and the freeway were separated only by a

wide-meshed fence. The other location was about 50 m away from the freeway in southeast direction (Site B). This site is still influenced by the presence of the freeway and, to a lesser extent, by urban background and possibly some local street traffic. The vehicle-generated particles have some time to age before being sampled at Site B.

Particle chemical composition was measured at two sites concurrently. The first site (Site A′) was on same side and at same distance (2.5 m) to the freeway as Site A, located at about 50 m northeast from Site A. The second site (Site B′) was chosen to represent local background, which is not or only weakly influenced by the freeway. The site was about 150 m east from Site A′, still in Hermon Park.

Traffic on SR 110 was free flowing during the whole sampling period. The traffic volume varied throughout the day, having a peak in the morning and one in the early evening corresponding to the rush hours. The morning rush hour is predominantly on the southbound lanes, while the evening rush hour is on the northbound lanes. The hourly averages of the total traffic density are shown in Figure 2. During the sampling period the average traffic density was about 5700 h^{-1}. Traffic speed was fairly constant during the day, and even during the rush hours the traffic did not slow down significantly. The average of the diurnal hourly averages was 108 $km \cdot h^{-1}$ on the southbound lanes, with a standard deviation of only 2.8 $km \cdot h^{-1}$; the average speed on the northbound lanes was 115 $km \cdot h^{-1}$ with a standard deviation of only 2.6 $km \cdot h^{-1}$.

The wind direction, wind speed, and temperature were monitored with a weather station (Wizard III, Weather Systems Company, San Jose, CA, USA) connected to a computer for data logging. Data were averaged over 5 min intervals. The wind direction was recorded as predominantly coming from one of 16 directions (22.5° intervals: namely north (N), north-northeast (NNE), northeast (NE), etc.) during the 5 min averaging period.

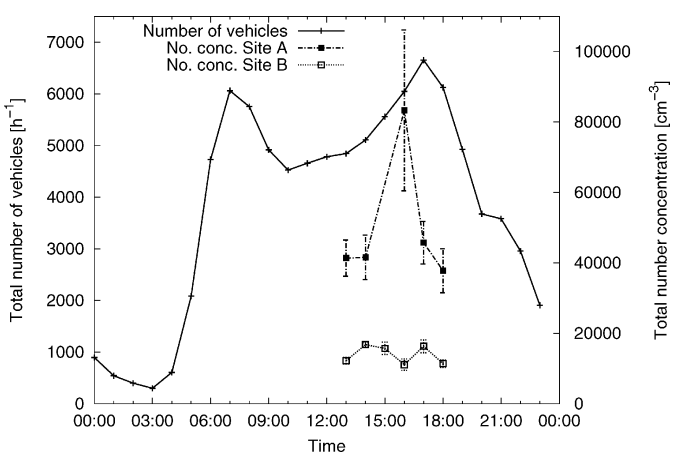

FIG. 2. Total traffic density and total number concentrations at Site A and Site B (SMPS integrals with standard errors). Hourly averages over the whole sampling period are shown. The values are shown at the begining of the averaged hour.

The wind vane was 2 m above ground level about 20 m southeast of SR 110 (close to Site A′).

The average temperature during the sampling period was 25°C (standard deviation of 5°C). The relative humidity was monitored using a Q-Trak Plus (TSI Inc., St. Paul, MN, USA) and it was 51% on average (standard deviation of all 1 min averages of 10%). The predominant wind direction during the sampling period was SW (29%), and 66% of the 5 min averages had predominant wind directions SSW, SW, or WSW. The average wind speed during the sampling period was 1.6 $m \cdot s^{-1}$ (standard deviation of 0.5 $m \cdot s^{-1}$). For Site A the wind direction is not very important, as here the sampling takes place close to the freeway where the air is mixed by turbulences created by the flowing traffic. Hence, the majority of the particles at this site originates from fresh vehicular emissions. At Site B, on the other hand, wind direction is likely to influence the aerosol mixture sampled. Differently aged aerosol from different stretches of the freeway upstream of the site mixed with background aerosol arrives at the site. On average, it is expected that results from this site will show effects caused by aging of freeway-generated aerosol.

Measurements of Particle Chemical Composition

A micro-orifice uniform deposit impactor (MOUDI; Model 110, MSP Corporation, Shoreview, MN, USA) sampled at 30 $l \cdot min^{-1}$ to collect particles on Teflon substrates for determination of mass concentrations. Collocated with the MOUDI, a modified high-volume sampler (Fine et al. 2004a) concurrently collected PM_{10} in three size ranges on quartz fiber substrates. The stages in the MOUDI were chosen to correspond to the same size cutpoints as the high-volume sampler: a coarse mode from 2.5 to 10 μm, an accumulation mode from 0.18 to 2.5 μm, and an ultrafine mode of particles less than 0.18 μm in aerodynamic diameter. The 47 mm Teflon filters from the MOUDI were pre- and postweighed after 24 h of equilibration at 45 to 50% relative humidity and a temperature range of 20–24°C. After weighing to determine particle mass concentration, filters were analyzed by X-ray fluorescence analysis (XRF) for metals and other trace elements (Dzubay 1977). Portions of the quartz fiber filters from the high-volume sampler were analyzed for elemental carbon and organic carbon (EC/OC) by thermal desorption/optical transmission analysis (Birch and Cary 1996). Additional portions of the quartz fiber filters were used to determine sulfate and nitrate concentrations by ion chromatography (Mueller et al. 1978).

Two 4.5 kW gasoline-powered portable generators provided the electric power for the pumps of MOUDI and high-volume samplers. The generators were placed approximately 20 m downwind of Site A′ and Site B′, so that no measurement could be biased by the generator's exhaust.

During the sampling period the MOUDI and high-volume sampler operated from 12 pm to 7 pm every day. The filters were deployed for several days. At both sites five periods were sampled: 17–21 May, 24–26 May, 27–28 May, 1–2 June, and 3–4 June 2004.

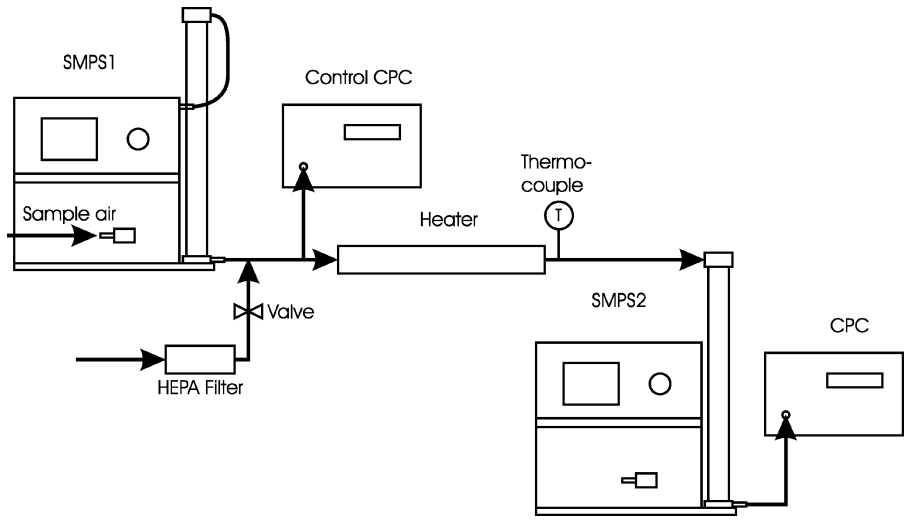

FIG. 3. Setup used for volatility measurements.

Particle Volatility Measurements

The TDMA system used to measure the volatility of particles is shown in Figure 3. The two scanning mobility particle sizers (SMPS; TSI model 3936) consisted of a bipolar charger (with an ^{85}Kr source), a long DMA (model 3081), and a condensation particle counter (CPC; TSI model 3022A). The first SMPS (SMPS1) sampled selected particles of a certain narrow size range from ambient aerosol. It operated with an aerosol flow rate of 1.5 $l \cdot min^{-1}$ and a sheath air flow rate of 15 $l \cdot min^{-1}$. Clean filtered air was introduced into the aerosol flow after size selection to increase its flow rate to 1.8 $l \cdot min^{-1}$. This monodisperse aerosol flow was split into two streams. One stream went into the CPC of SMPS1 (control CPC, sample flow rate of 0.3 $l \cdot min^{-1}$), which measured the concentration of this monodisperse aerosol. The other stream traveled through a heater unit, where the aerosol was conditioned to a certain fixed temperature. After passing through the heater, the aerosol went through DMA2 (DMA of the second SMPS, SMPS2) without passing through the bipolar charger. SMPS2 (in scanning mode) measured the size distribution of the conditioned aerosol and was operated with a CPC aerosol flow rate of 1.5 $l \cdot min^{-1}$ and a sheath air flow rate of 15 $l \cdot min^{-1}$. Two computers were used for data logging from control CPC and SMPS2.

The heater used to condition the aerosol is described in Kuhn et al. (2005). The Aerosol Instrument Manager software (version 5.2, TSI Inc., St. Paul, MN, USA) was used for inversion of the measured number concentrations (CPC of SMPS2) to the size distribution. It was assumed that particles did not lose their charge during heating and evaporation of the volatile fraction; therefore, all particles were still charged (as by electrostatic size selection by SMPS1) when they entered DMA2. This assumption was justified by looking at the ratio of particles remaining after heating, which was close to 1 when all particles had sizes above the detection limit of SMPS2 (see Section "Volatility Comparisons" below). The electric power for the instruments was provided by four lead batteries and an inverter (ProSine 2.0, 2 kW inverter and charger).

Measurements of volatility were conducted at both Site A and Site B. During a typical measurement cycle at one site, a certain particle size was fixed and the size distribution measured at ambient temperature and after conditioning at two different heated temperatures. A measurement cycle was concluded by measuring the full size distribution of the ambient aerosol directly (DMA of SMPS1 bypassed and heater turned off). Up to three measurement cycles were carried out each day, of which the last was started after 4 pm, to capture the evening rush-hour condition. For each selected particle size two or three measurement cycles were carried out on different days, of which one was during the evening rush hour.

Four particle diameters were chosen within the ultrafine size range: 20, 40, 80, and 120 nm. For heating, aerosol flow temperatures of 60°C and 110°C were chosen to determine ultrafine particle volatility. We expected most of the volatile material to evaporate at 110°C (Philippin et al. 2004), and we selected this temperature so that we could compare results with our previous study (Kuhn et al. 2005) close to a mixed heavy- and light-duty traffic freeway. The temperature of 60°C was selected to represent an intermediate state of volatilization.

Measurements of size distributions were repeated three to six times while the aerosol temperature was kept constant. Each size distribution was measured with 81 SMPS channels from 8.2 to 146 nm (midpoint diameters). The size distribution was measured in scanning mode by SMPS2 in 162 s; consequently, each SMPS channel was sampled for 2 s. The control CPC was used with an averaging time of 2 s. The control CPC data could therefore be used to normalize the SMPS data by dividing the value of each channel by the control CPC concentration at the same time that the channel was scanned.

The repeated measurements of distributions at same conditions showed variations caused, at Site A, by the extreme vicinity to the source (freeway traffic) and its temporal variations. At Site B, the source is more distant and variations here are caused by temporal changes of the source as well as by local wind conditions changing the aerosol mixture sampled at the site. However, the average of these repeated measurements are similar to averages of measurements taken at different times of the day or on a different day. Therefore, the average of all measurements at a given site, sampled particle size, and conditioning temperature was used for comparison with averages at different site, size, or temperature.

RESULTS AND DISCUSSION

Particle Chemical Composition

Table 1 shows the results from the chemical analysis of the MOUDI and high-volume sampler filters and substrates from the two sites. At Site A′, directly next to the freeway, mass concentrations in the coarse and accumulation size ranges were similar to Site B′, whereas ultrafine mass concentration was higher at Site A′. Nitrate was found in similar concentrations in the accumulation mode but showed higher concentrations in the coarse and ultrafine modes next to the freeway (Site A′). Sulfate, on the other hand, was similar in the coarse and accumulation

TABLE 1
PM_{10} size fractionated, chemically speciated data

	Coarse		Accum.		Ultrafine			Coarse		Accum.		Ultrafine	
	A′	B′	A′	B′	A′	B′		A′	B′	A′	B′	A′	B′
Mass							K						
Mean	23.000	21.457	18.995	19.194	5.113	3.268	Mean	0.360	0.711	0.024	0.023	0.023	0.038
SD	7.912	7.569	9.492	6.082	1.729	1.490	SD	0.099	0.216	0.004	0.007	0.005	0.036
Nitrate							Ca						
Mean	1.855	1.387	1.889	2.069	1.090	0.737	Mean	0.847	1.663	0.033	0.031	0.041	0.083
SD	0.837	0.357	1.407	1.253	0.204	0.246	SD	0.222	0.628	0.005	0.011	0.009	0.092
Sulfate							Ti						
Mean	0.570	0.547	2.727	3.560	1.748	2.352	Mean	0.136	0.197	0.008	0.005	0.011	0.012
SD	0.202	0.144	1.569	2.251	0.579	0.659	SD	0.043	0.084	0.001	0.001	0.003	0.012
OC							V						
Mean	0.638	0.807	2.529	2.167	7.387	6.080	Mean	0.009	0.008	0.005	0.005	0.002	0.001
SD	0.117	0.267	1.142	0.831	1.912	2.061	SD	0.003	0.007	0.001	0.002	0.001	0.001
EC							Fe						
Mean	0.031	0.038	0.198	0.118	1.109	0.663	Mean	1.971	2.447	0.123	0.061	0.124	0.120
SD	0.007	0.017	0.216	0.104	0.558	0.235	SD	0.648	0.916	0.009	0.023	0.032	0.115
Na							Ni						
Mean	0.734	1.148	0.034	0.039	0.002	0.016	Mean	0.001	0.003	0.002	0.002	0.000	0.000
SD	0.123	0.264	0.008	0.013	0.002	0.015	SD	0.000	0.001	0.001	0.001	0.000	0.000
Mg							Cu						
Mean	0.124	0.239	0.003	0.003	0.003	0.006	Mean	0.081	0.054	0.007	0.002	0.006	0.002
SD	0.027	0.055	0.002	0.003	0.003	0.006	SD	0.027	0.021	0.001	0.001	0.002	0.002
Al							Zn						
Mean	0.325	0.775	0.008	0.011	0.033	0.065	Mean	0.039	0.059	0.009	0.008	0.006	0.007
SD	0.121	0.267	0.004	0.008	0.005	0.064	SD	0.013	0.029	0.004	0.004	0.003	0.006
Si							Ba						
Mean	1.039	2.449	0.032	0.087	0.104	0.209	Mean	0.105	0.159	0.014	0.004	0.011	0.006
SD	0.384	0.853	0.010	0.117	0.014	0.204	SD	0.057	0.043	0.003	0.003	0.006	0.008
S							Sb						
Mean	0.640	1.021	0.533	0.593	0.260	0.299	Mean	0.011	0.012	0.001	0.001	0.001	0.001
SD	0.306	0.358	0.164	0.161	0.229	0.259	SD	0.008	0.008	0.001	0.001	0.001	0.001
Cl							Pb						
Mean	1.154	1.676	0.046	0.042	0.004	0.019	Mean	0.008	0.021	0.002	0.001	0.001	0.002
SD	0.501	0.755	0.033	0.033	0.002	0.028	SD	0.007	0.011	0.001	0.001	0.001	0.001

All mass concentrations are given in $\mu g \cdot m^{-3}$.

modes, while the ultrafine mode concentration was somewhat higher away from the freeway (Site B′).

Interestingly, the elemental mass concentrations in the coarse size range were either similar or higher at Site B′ (higher for Na, Mg, Al, Si, S, Cl, K, Ca, Ni, Zn, and Ba). Exceptions, where coarse concentrations were higher at Site A′, were nitrate and copper. This trend in the coarse PM concentrations between the two sites suggests that light-duty vehicles may not be a significant source of coarse particles. This is consistent with the findings of Sternbeck et al. (2002) and Charron and Harrison (2003), who showed that heavy-duty vehicles generate higher amounts of coarse PM due to stronger abrasion processes, including tire wear and brake linings. Sternbeck et al. (2002) showed that a higher correlation exists between particle barium, a common element in brake linings, and heavy-duty traffic than light-duty traffic. In addition, contributions from brake wear are likely to be very small at SR 110 because of the steady speed conditions, with very little braking happening during the sampling period. With only a few exceptions (Fe being the most prominent), the accumulation mode concentrations were similar at both sites, thereby confirming that this size range represents for the most part a background urban aerosol, unaffected by local traffic.

In the ultrafine size range, the most noticeable difference was observed for mass, nitrate, and EC concentrations, which were higher at Site A′, possibly reflecting the effect of light-duty emissions. Most other species occurred in similar concentrations in the ultrafine mode. Vanadium and copper were also higher at Site A′ but were present in concentrations close to the uncertainty level at Site B′. Sulfate, sodium, and titanium were higher at Site B′. In the case of OC in the ultrafine mode, unreasonably high concentrations were measured, often exceeding the total ultrafine mass concentration. This is caused by adsorption of organic vapors, which in the ultrafine size range become large in relation to the relatively low amount of particulate matter collected on the filter (Mader and Pankow 2001). This phenomenon is not expected to affect the coarse and accumulation modes as drastically since these particle size ranges were collected by impaction onto substrates and not by filtration. Therefore, the actual ultrafine particle OC content remains unknown, although other studies have shown that ultrafine gasoline vehicle emissions are primarily composed of OC (Kleeman et al. 2000).

Number, Surface, and Mass Concentrations

Integrating the SMPS size distributions of ambient aerosol of the two sites yields number, surface, and volume concentrations. Mass concentration can be estimated from volume concentration assuming a certain density. Mass concentration measured in the ultrafine mode of the MOUDI can be compared to the SMPS volume concentration. Table 2 shows the values found in this study.

Differences between the calculated SMPS and the measured ultrafine MOUDI mass concentrations may result from losses of volatile and semivolatile materials from the MOUDI filters before analysis, which would result in reduced MOUDI mass. Deviations of the shape of the particles from spherical may also result in differences in mass concentrations due to the different sizing techniques (McMurry et al. 2002; Park et al. 2003; Shen et al. 2002). In addition, the particle bounce problem, which causes larger particles to be collected in lower stages of the MOUDI, might result in overestimated MOUDI ultrafine mass. Shen et al. (2002) observed in the ultrafine range a higher MOUDI than SMPS mass.

Size Distribution of Ambient Aerosol

All measured size distributions of ambient aerosol from each site were averaged, as shown in Figure 4. The size distribution next to the freeway (Site A) shows two modes at about 10 and 20 nm. Two modes below 30 nm were also found at the Interstates 710 (I-710) and 405 (I-405), with 25 and 7% heavy-duty vehicles, respectively, in Los Angeles, CA during studies conducted under similar meteorological conditions in the summer season (Zhu et al. 2002a, 2002b). These modes might arise from nucleation of semivolatiles very near the vehicle tailpipe.

There is also a less pronounced mode at 50 nm in the size distribution at Site A. At 60 and 90 m distance from I-405, Zhu et al. (2002b) found a dominant mode at about 40 nm. This, as well as the 50 nm mode in this study might be explained by condensational growth (Zhang et al. 2004a). With the wind direction predominantly parallel to the freeway, such growth could occur while the aging particles remain close to the freeway. At Site B no modes can be seen, indicating that the modes at Site A are characteristic of the freeway-generated aerosol. Dilution and mixing with urban background yield the lower concentrations at Site B.

TABLE 2
SMPS total number, surface, and volume concentrations are shown

Site	Number cm^{-3}	SD cm^{-3}	Surface $\mu m^2 \cdot cm^{-3}$	Volume $\mu m^3 \cdot cm^{-3}$	Mass $\mu g \cdot m^{-3}$	MOUDI $\mu g \cdot m^{-3}$
Site A	46 000	29 800	65.0	3.57	5.71	6.32
Site B	13 600	4 680	18.6	0.995	1.59	2.49

Surface and volume concentrations were calculated assuming spherical particles. For conversion to mass a density of 1 600 $kg \cdot m^{-3}$ was used. MOUDI ultrafine mass concentrations are shown as comparison; MOUDI mass (from the third week only) at Site A′ is compared to Site A, Site B′ (second week only) to Site B.

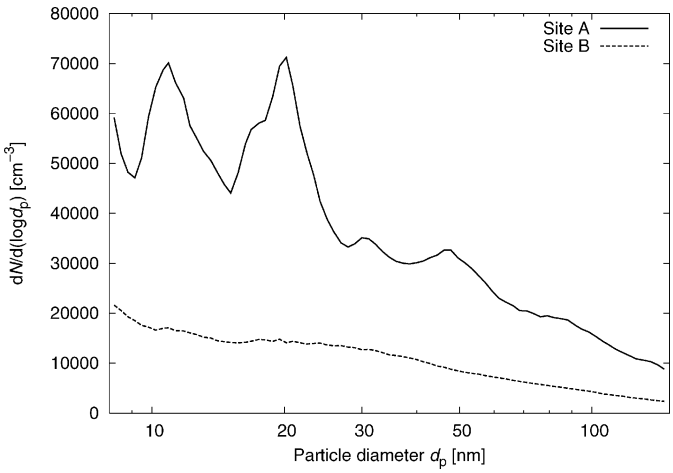

FIG. 4. Average size distributions of ambient aerosol. At Site A results from eight measurement cycles (each containing six size distributions) were averaged. At Site B eleven measurement cycles were averaged.

Despite these similarities of distributions at Site A to freeways with up to 25% heavy-duty vehicles, the number concentrations are significantly lower at SR 110. This difference cannot be accounted for only by the difference in traffic volume between the two freeways, which suggests that heavy-duty vehicles emit higher particle number concentrations than light-duty vehicles (Kittelson et al. 2004).

Volatility Properties

Size Distribution Changes

Figure 5 shows averaged results from volatility measurements. For each selected particle size at both sites, three normalized number size distributions are shown: the first represents the selected monodisperse aerosol at ambient temperature without conditioning (no heating); the second shows the size distribution after heating to 60°C; the third after heating to 110°C. The presented size distributions are averaged over all measurements.

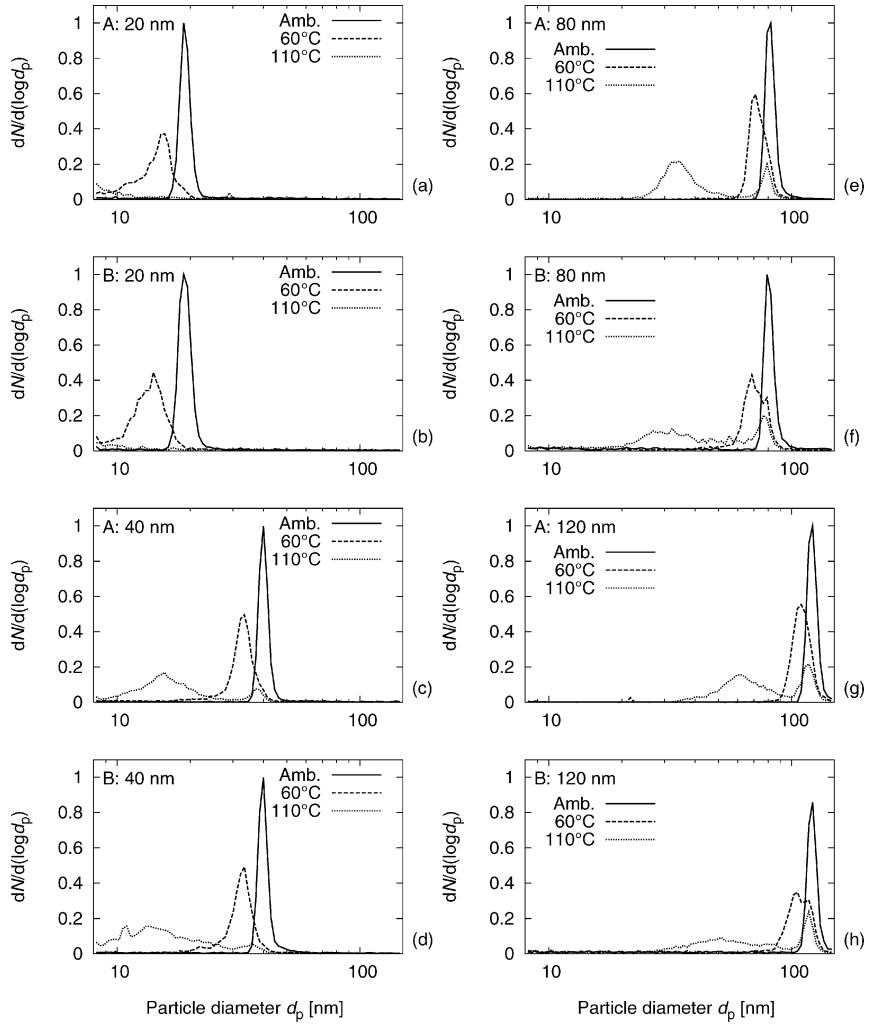

FIG. 5. Average number size distribution (normalized to maximum at 1) at ambient temperature (≈25°C) and after conditioning (heating) at 60°C and 110°C. (a) 20 nm aerosol at Site A, (b) 20 nm at Site B, (c) 40 nm at Site A, (d) 40 nm at Site B, (e) 80 nm at Site A, (f) 80 nm at Site B, (g) 120 nm at Site A, and (h) 120 nm at Site B.

The diameter of each measured particle size shrank when heated. This resulted in a decrease of the mode diameter d_m (mode decrease Δd_m) from the original size of the monodisperse aerosol towards much smaller diameters. The distribution also broadened when the aerosol was heated. This broadening effect is stronger at Site B, because the aerosol originating from freeway traffic is diluted and mixed with particles from multiple other sources with a wider range of volatility characteristics. At Site A (next to the freeway) the aerosol originates mainly from freeway traffic and hence most particles of a given size have similar characteristics.

For the 80 and 120 nm aerosols the unimodal distributions split into bimodal distributions upon heating to 110°C. In each case a mode exists at the original (before heating) particle diameter, and a new mode with a wider range forms at a smaller diameter. This indicates that these aerosols are externally mixed, that is, each aerosol consists of two groups of particles having very different volatilities. Highly volatile particles lose a significant fraction of volume to the vapor phase, as is demonstrated by the mode that decreased significantly in diameter. These particles are designated *mostly volatile* because volatile material dominates their compositions. Particles that, on the other hand, do not shrink significantly contribute to the mode that remains near the original diameter. Those particles will be referred to as *nonvolatile*.

As described by Kuhn et al. (2005), the ratios ϕ_N and ϕ_V can be used to describe the relative amount of number and volume that remains after heating the aerosol. The extent of external mixing can be described by the ratio ($\phi_{N\mathrm{n}}$) of the integral of the nonvolatile mode of the normalized number size distribution at 110°C to the integral of the normalized distribution at ambient temperature. This ratio gives the fraction of the aerosol that is nonvolatile and can be calculated as

$$\phi_{N\mathrm{n}} = \frac{\int_C^U n_{110^\circ\mathrm{C}} \mathrm{d}(\log d_\mathrm{p})}{\int_L^U n_\mathrm{amb} \mathrm{d}(\log d_\mathrm{p})}$$

where L and U are the lower and upper limit of the size range of SMPS2, C is a cut size between the mostly volatile and nonvolatile modes, and n_amb and $n_{110^\circ\mathrm{C}}$ are the normalized size distributions at ambient temperature and 110°C. In addition, the new ratios $\psi_{N\mathrm{m}}$ for number and $\psi_{V\mathrm{m}}$ for volume concentrations were introduced to characterize the relative amount of the mostly volatile component that remains after heating of the aerosol. Assuming that there are no number losses of nonvolatile particles, the fraction of mostly volatile particles (before losses) can be calculated as $1-\phi_{N\mathrm{n}}$. The ratio $\psi_{N\mathrm{m}}$ is then $\psi_{N\mathrm{m}} = \phi_{N\mathrm{m}}/(1-\phi_{N\mathrm{n}})$, where $\phi_{N\mathrm{m}}$ is the ratio of the integral of the mostly volatile mode at 110°C to the integral of the distribution at ambient temperature (defined like $\phi_{N\mathrm{n}}$, but for the mostly volatile mode). The ratio $\psi_{V\mathrm{m}}$ is calculated as $\psi_{V\mathrm{m}} = \phi_{V\mathrm{m}}/(1-\phi_{N\mathrm{n}})$, where $\phi_{V\mathrm{m}}$ is the ratio of the integral of the mostly volatile volume mode at 110°C to the integral of the volume distribution at ambient temperature (like $\phi_{N\mathrm{m}}$, but calculated using volume size distribution).

The 40 nm aerosol, at both Site A and Site B, had only a very small nonvolatile mode at 110°C. This indicates that it is externally mixed, but the fraction of nonvolatile particles is very small compared to the 80 and 120 nm aerosols. To determine $\phi_{N\mathrm{n}}$, the following size cuts between nonvolatile and mostly volatile modes were used as estimated from the shape of the size distributions at 110°C: $d_\mathrm{p} \geq 31.1$ nm for the nonvolatile mode of 40 nm aerosol, ≥63.8 nm for 80 nm, and ≥102 nm for 120 nm. The values of $\phi_{N\mathrm{n}}$ (± Std. Dev.) for 40, 80, and 120 nm are 0.059 (± 0.029), 0.20 (± 0.19), and 0.28 (± 0.14), respectively, at Site A. The values at Site B are 0.10 (± 0.06), 0.25 (± 0.08), and 0.24 (± 0.06).

The 20 nm aerosol does not show external mixing on the size distributions at 110°C. This suggests that the vast majority of the 20 nm particles is semivolatile. Hence, the 20 nm aerosol is only internally mixed, and the particles are composed mainly of volatile material and may or may not contain some material that is not volatile (such as a solid core, the size of which may be smaller than the lower sizing limit of the SMPS, which in our experiments was 8 nm). This is essentially the same at both sites and was also found by Kuhn et al. (2005). For diesel exhaust, Sakurai et al. (2003b) found a solid core below about 8 nm for 30 nm particles and below 4 nm for 12 nm particles.

Temperature Dependence

The temperature dependence of the mode decrease Δd_m at Site A is shown as a thermal desorption profile in Figure 6. This study shows larger decreases in mode diameters than a similar study that took place at I-405 in winter 2003/2004 at 15 m distance to the freeway (Kuhn et al. 2005). The difference would probably be even larger if one considered seasonal effects on volatility (the volatile fraction of PM would increase in winter

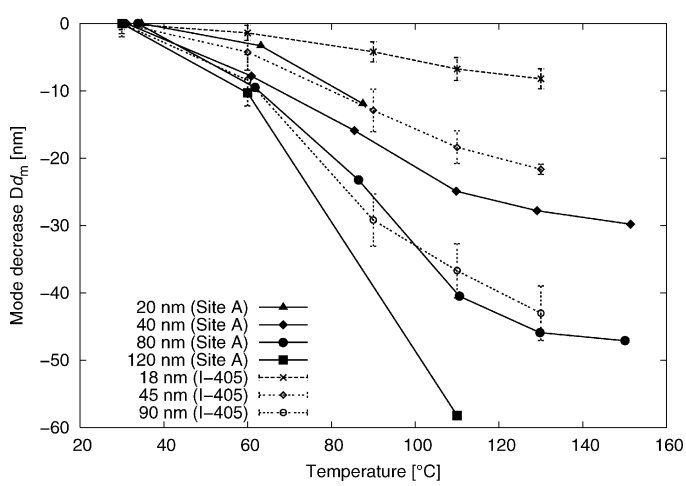

FIG. 6. The temperature dependence of the mode decrease Δd_m is shown for 20, 40, 80, and 120 nm aerosols at Site A (next to SR 110). For comparison, the mode decrease for 18, 45, and 90 nm aerosols at the I-405 (Kuhn et al. 2005), measured in winter 2003/2004 at 15 m distance to the freeway is shown.

due to colder temperatures). Hence, aerosols originating from gasoline traffic seem to be substantially more volatile in comparison to aerosols dominated by a mixture of heavy- and light-duty vehicles.

The mode decrease was similar at both sites of this study, with the mode diameters decreasing slightly more at Site B than at Site A (see Figure 5). This suggests that particle volatility properties do not change significantly from Site A to Site B.

Volatility Comparisons

To examine particle volatility further, the ratios ϕ_N, ϕ_V, $\psi_{N\mathrm{m}}$, and $\psi_{V\mathrm{m}}$ have been calculated from the integrals of the size distributions at ambient temperature, 60°C, and 110°C. The values of ϕ_N and ϕ_V at Site A and Site B are reported in Figure 7, and $\psi_{N\mathrm{m}}$ and $\psi_{V\mathrm{m}}$ in Figure 8. As Figures 7 and 8 show, in most cases heating did not result in significant particle number losses. Only 20 nm particles heated to 110°C were lower in number concentrations than those at ambient temperature. This may be due to shrinkage to sizes below the CPC's detection limit of 8 nm.

All ratios at Site B are similar to those at Site A. Also the fractions $\phi_{N\mathrm{n}}$ are similar, indicating that at the two sites the same fraction of the aerosol is nonvolatile. From Site A to Site B only the concentrations (number and volume, see Table 2) change significantly, while the average volatility remains relatively similar for any given particle size studied. However, particles that grow to larger sizes by condensation of volatile material might increase volatility as compared to particles that already have a larger size shortly after emission. This could be the reason for a slightly larger mode decrease observed for 120 nm particles at Site B ($\Delta d_{\mathrm{m}} = -67$ nm) compared to Site A (-58 nm) and higher volume losses at Site B ($\psi_{V\mathrm{m}} = 0.11 \pm 0.02$) compared to Site A ($0.14 \pm 0.03$).

The volatility data from SR 110 was compared to data at the I-405 collected in winter 2003/2004 (Kuhn et al. 2005). The fractions $\phi_{N\mathrm{n}}$ for data at I-405 were 17% for both 45 nm and 90 nm. This indicates that at SR 110 a lower fraction of particles in the range from 40 to 45 nm and a similar fraction of particles in the range from 80 to 90 nm are nonvolatile. The higher fraction of nonvolatile particles at the I-405 might originate, in part, from the diesel vehicles on that freeway (Sakurai et al. 2003a).

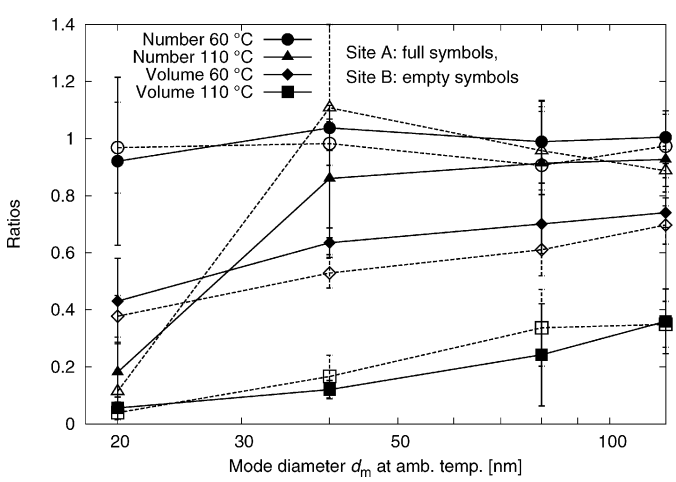

FIG. 7. Number and volume concentration ratios ϕ_N and ϕ_V at Site A and Site B at 60°C and 110°C.

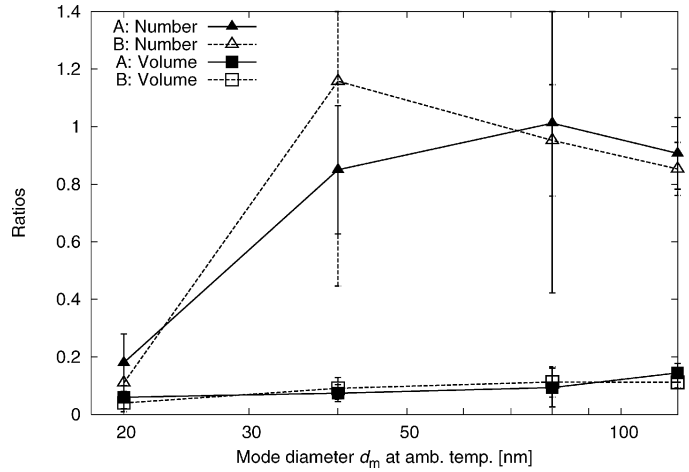

FIG. 8. Number and volume concentration ratios $\psi_{N\mathrm{m}}$ and $\psi_{V\mathrm{m}}$ at Site A and Site B. Values shown for 20 nm aerosol are from ϕ_N and ϕ_V, as no external mixing can be observed.

CONCLUSIONS

The volatile material content of ultrafine particles, as well as mass concentration and chemical composition of ultrafine, accumulation, and coarse PM were measured at the edge of a freeway with only gasoline vehicles. The number concentrations were relatively low at SR 110 as compared to freeways with mixed diesel and gasoline traffic. This may be due to lower emissions, in terms of ultrafine number concentration, of gasoline vehicles.

The MOUDI ultrafine mass concentration, nitrate, and EC were higher at Site A′, which may result from the freeway emissions. The other components analyzed in the ultrafine mode had similar concentrations next to the freeway and at the background site (Site B′). In the coarse size range, on the other hand, mass concentration was similar at both sites, and most other components were either higher at Site B′ (e.g., Na, Si, and Ba) or similar in concentration, which might suggest that light-duty vehicles may not be a significant source of coarse particles.

The volatility properties at the two sites were similar on average. Relatively high volatility was found, with about 65% of volume of 120 nm particles lost when heated to 110°C, and about 95% of volume of 20 nm particles. Compared to particles from a mixed heavy- and light-duty freeway, aerosol originating from gasoline traffic in this study had a stronger mode decrease. After heating to 110°C particles shrank on average to about half their original size. Heating the particles more resulted in further decrease of their size or loss of particles as they shrank below the lower detection limit of the DMA, which was 8 nm in this study.

For aerosols of 40 nm particles and above external mixing was observed, with a nonvolatile fraction of up to 28% for 120 nm aerosol. This fraction increases with increasing mode diameter of the aerosol.

REFERENCES

Allen, J. O., Mayo, P. R., Hughes, L. S., Salmon, L. G., and Cass, G. R. (2001). Emissions of Size-Segregated Aerosols from On-Road Vehicles in the Caldecott Tunnel, *Environ. Sci. Technol.* 35(21):4189–4197.

Birch, M. E., and Cary, R. A. (1996). Elemental Carbon-Based Method for Monitoring Occupational Exposures to Particulate Diesel Exhaust, *Aerosol Sci. Technol.* 25(3):221–241.

Charron, A., and Harrison, R. M. (2003). Primary Particle Formation from Vehicle Emissions During Exhaust Dilution in the Roadside Atmosphere, *Atmos. Environ.* 37(29):4109–4119.

Chase, R. E., Duszkiewicz, G. J., Jensen, T. E., Lewis, D., Schlaps, E. J., Weibel, A. T., Cadle, S., and Mulawa, P. (2000). Particle Mass Emission Rates from Current-Technology, Light-Duty Gasoline Vehicles, *J. Air Waste Manage. Assoc.* 50(6):930–935.

Donaldson, K., Brown, D., Clouter, A., Duffin, R., MacNee, W., Renwick, L., Tran, L., and Stone, V. (2002). The Pulmonary Toxicology of Ultrafine Particles, *J. Aerosol Med.* 15(2):213–220.

Dzubay, T. G. (1977). *X-ray Fluorescence Analysis of Environmental Samples*, Ann Arbor Science Publishers, Ann Arbor, MI.

Fine, P. M., Chakrabarti, B., Krudysz, M., Schauer, J. J., and Sioutas, C. (2004a). Diurnal Variations of Individual Organic Compound Constituents of Ultrafine and Accumulation Mode Particulate Matter in the Los Angeles Basin, *Environ. Sci. Technol.* 38(5):1296–1304.

Fine, P. M., Shen, S., and Sioutas, C. (2004b). Inferring the Sources of Fine and Ultrafine Particulate Matter at Downwind Receptor Sites in the Los Angeles Basin Using Multiple Continuous Measurements, *Aerosol Sci. Technol.* 38:182–195.

Fraser, M. P., Cass, G. R., and Simoneit, B. R. T. (1998). Gas-Phase and Particle-Phase Organic Compounds Emitted from Motor Vehicle Traffic in a Los Angeles Roadway Tunnel, *Environ. Sci. Technol.* 32(14):2051–2060.

Harrison, R. M., Tilling, R., Romero, M. S. C., Harrad, S., and Jarvis, K. (2003). A Study of Trace Metals and Polycyclic Aromatic Hydrocarbons in the Roadside Environment, *Atmos. Environ.* 37(17):2391–2402.

Hitchins, J., Morawska, L., Wolff, R., and Gilbert, D. (2000). Concentrations of Submicrometre Particles from Vehicle Emissions Near a Major Road, *Atmos. Environ.* 34(1):51–59.

Holmen, B. A., and Qu, Y. G. (2004). Uncertainty in Particle Number Modal Analysis During Transient Operation of Compressed Natural Gas, Diesel, and Trap-Equipped Diesel Transit Buses, *Environ. Sci. Technol.* 38(8):2413–2423.

Kittelson, D. B., Watts, W. F., and Johnson, J. P. (2004). Nanoparticle Emissions on Minnesota Highways, *Atmos. Environ.* 38(1):9–19.

Kleeman, M. J., Schauer, J. J., and Cass, G. R. (2000). Size and Composition Distribution of Fine Particulate Matter Emitted from Motor Vehicles, *Environ. Sci. Technol.* 34(7):1132–1142.

Kuhn, T., Krudysz, M., Zhu, Y., Fine, P. M., Hinds, W. C., Froines, J., and Sioutas, C. (2005). Volatility of Indoor and Outdoor Ultrafine Particulate Matter Near a Freeway, *J. Aerosol Sci.* 36(3):291–302.

Kwon, S. B., Lee, K. W., Saito, K., Shinozaki, O., and Seto, T. (2003). Size-Dependent Volatility of Diesel Nanoparticles: Chassis Dynamometer Experiments, *Environ. Sci. Technol.* 37(9):1794–1802.

Laschober, C., Limbeck, A., Rendl, J., and Puxbaum, H. (2004). Particulate Emissions from On-Road Vehicles in the Kaisermühlen-Tunnel (Vienna, Austria), *Atmos. Environ.* 38(14):2187–2195.

Li, N., Sioutas, C., Cho, A., Schmitz, D., Misra, C., Sempf, J., Wang, M., Oberley, T., Froines, J., and Nel, A. (2003). Ultrafine Particulate Pollutants Induce Oxidative Stress and Mitochondrial Damage, *Environ. Health Perspect.* 111(4):455–460.

Lyyranen, J., Jokiniemi, J., Kauppinen, E. I., Backman, U., and Vesala, H. (2004). Comparison of Different Dilution Methods for Measuring Diesel Particle Emissions, *Aerosol Sci. Technol.* 38(1):12–23.

Mader, B. T., and Pankow, J. F. (2001). Gas/Solid Partitioning of Semivolatile Organic Compounds (SOCs) to Air Filters. 3. An Analysis of Gas Adsorption Artifacts in Measurements of Atmospheric SOCs and Organic Carbon (OC) when Using Teflon Membrane Filters and Quartz Fiber Filters, *Environ. Sci. Technol.* 35(17):3422–3432.

McGaughey, G. R., Desai, N. R., Allen, D. T., Seila, R. L., Lonneman, W. A., Fraser, M. P., Harley, R. A., Pollack, A. K., Ivy, J. M., and Price, J. H. (2004). Analysis of Motor Vehicle Emissions in a Houston Tunnel During the Texas Air Quality Study 2000, *Atmos. Environ.* 38(20):3363–3372.

McMurry, P. H., Wang, X., Park, K., and Ehara, K. (2002). The Relationship Between Mass and Mobility for Atmospheric Particles: A New Technique for Measuring Particle Density, *Aerosol Sci. Technol.* 36(2):227–238.

Morawska, L., Bofinger, N. D., Kocis, L., and Nwankwoala, A. (1998). Submicrometer and Supermicrometer Particles from Diesel Vehicle Emissions, *Environ. Sci. Technol.* 32(14):2033–2042.

Mueller, P. K., Mendoza, B. V., Collins, J. C., and Wilgus, E. A. (1978). Application of Ion Chromatography to the Analysis of Anions Extracted from Airborne Particulate Matter. In *Ion Chromatographic Analysis of Environmental Pollutants*, edited by E. Sawicki, J. D. Mulik, and E. Wittgenstein, Ann Arbor Science Publishers, Ann Arbor, MI, pp. 77–86.

National Research Council. (2004). *Research Priorities for Airborne Particulate Matter: IV. Continuing Research Progress.* Committee on Research Priorities for Airborne Particulate Matter, National Research Council, Washington, DC.

Oberdörster, G. (2000). Toxicology of Ultrafine Particles: In Vivo Studies, *Philos. Trans. Royal Soc. London Series A—Math. Phys. Eng. Sci.* 358(1775):2719–2739.

Park, K., Cao, F., Kittelson, D. B., and McMurry, P. H. (2003). Relationship between Particle Mass and Mobility for Diesel Exhaust Particles, *Environ. Sci. Technol.* 37(3):577–583.

Philippin, S., Wiedensohler, A., and Stratmann, F. (2004). Measurements of Non-Volatile Fractions of Pollution Aerosols with an Eight-Tube Volatility Tandem Differential Mobility Analyzer (VTDMA-8), *J. Aerosol Sci.* 35(2):185–203.

Pietropaoli, A. P., Frampton, M. W., Hyde, R. W., Morrow, P. E., Oberdörster, G., Cox, C., Speers, D. M., Frasier, L. M., Chalupa, D. C., Huang, L. S., and Utell, M. J. (2004). Pulmonary Function, Diffusing Capacity, and Inflammation in Healthy and Asthmatic Subjects Exposed to Ultrafine Particles, *Inhal. Toxicol.* 16:59–72.

Ristovski, Z. D., Morawska, L., Bofinger, N. D., and Hitchins, J. (1998). Submicrometer and Supermicrometer Particulate Emission from Spark Ignition Vehicles, *Environ. Sci. Technol.* 32(24):3845–3852.

Sakurai, H., Park, K., McMurry, P. H., Zarling, D. D., Kittelson, D. B., and Ziemann, P. J. (2003a). Size-Dependent Mixing Characteristics of Volatile and Nonvolatile Components in Diesel Exhaust Aerosols, *Environ. Sci. Technol.* 37(24):5487–5495.

Sakurai, H., Tobias, H. J., Park, K., Zarling, D., Docherty, S., Kittelson, D. B., McMurry, P. H., and Ziemann, P. J. (2003b). On-Line Measurements of Diesel Nanoparticle Composition and Volatility, *Atmos. Environ.* 37(9–10):1199–1210.

Schauer, J. J., Kleeman, M. J., Cass, G. R., and Simoneit, B. R. T. (1999). Measurement of Emissions from Air Pollution Sources. 2. C-1 Through C-30 Organic Compounds from Medium Duty Diesel Trucks, *Environ. Sci. Technol.* 33(10):1578–1587.

Schauer, J. J., Kleeman, M. J., Cass, G. R., and Simoneit, B. R. T. (2002). Measurement of Emissions from Air Pollution Sources. 5. C-1-C-32 Organic Compounds from Gasoline-Powered Motor Vehicles, *Environ. Sci. Technol.* 36(6):1169–1180.

Shah, S. D., Cocker, D. R., Miller, J. W., and Norbeck, J. M. (2004). Emission Rates of Particulate Matter and Elemental and Organic Carbon from In-Use Diesel Engines, *Environ. Sci. Technol.* 38(9):2544–2550.

Shen, S., Jaques, P. A., Zhu, Y., Geller, M. D., and Sioutas, C. (2002). Evaluation of the SMPS-APS System as a Continuous Monitor for Measuring PM2.5,

PM10 and Coarse (PM2.5-10) Concentrations, *Atmos. Environ.* 36(24):3939–3950.

Sternbeck, J., Sjodin, A., and Andreasson, K. (2002). Metal Emissions from Road Traffic and the Influence of Resuspension—Results from Two Tunnel Studies, *Atmos. Environ.* 36(30):4735–4744.

Sturm, P. J., Baltensperger, U., Bacher, M., Lechner, B., Hausberger, S., Heiden, B., Imhof, D., Weingartner, E., Prevot, A. S. H., Kurtenbach, R., and Wiesen, P. (2003). Roadside Measurements of Particulate Matter Size Distribution, *Atmos. Environ.* 37(37):5273–5281.

Suess, D. T., and Prather, K. A. (2002). Reproducibility of Single Particle Chemical Composition During a Heavy Duty Diesel Truck Dynamometer Study, *Aerosol Sci. Technol.* 36(12):1139–1141.

Vaaraslahti, K., Virtanen, A., Ristimäki, J., and Keskinen, J. (2002). Nucleation Mode Formation in Heavy-Duty Diesel Exhaust with and without a Particulate Filter, *Environ. Sci. Technol.* 38(18):4884–4890.

Vogt, R., Scheer, V., Casati, and R., Benter, T. (2003). On-Road Measurement of Particle Emission in the Exhaust Plume of a Diesel Passenger Car, *Environ. Sci. Technol.* 37(18):4070–4076.

Zhang, K. M., Wexler, A. S., Zhu, Y. F., Hinds, W. C., and Sioutas, C. (2004a). Evolution of Particle Number Distribution Near Roadways. Part II: the 'Road-to-Ambient' Process, *Atmos. Environ.* 38(38):6655–6665.

Zhang, Q., Stanier, C. O., Canagaratna, M. R., Jayne, J. T., Worsnop, D. R., Pandis, S. N., and Jimenez, J. L., (2004b). Insights into the Chemistry of New Particle Formation and Growth Events in Pittsburgh Based on Aerosol Mass Spectrometry, *Environ. Sci. Technol.* 38(18):4797–4809.

Zhu, Y. F., Hinds, W. C., Kim, S., Shen, S., and Sioutas, C. (2002a). Study of Ultrafine Particles Near a Major Highway with Heavy-Duty Diesel Traffic, *Atmos. Environ.* 36(27):4323–4335.

Zhu, Y. F., Hinds, W. C., Kim, S., and Sioutas, C. (2002b). Concentration and Size Distribution of Ultrafine Particles Near a Major Highway, *J. Air Waste Manage. Assoc.* 52(9):1032–1042.

Zhu, Y. F., Hinds, W. C., Shen, S., and Sioutas, C. (2004). Seasonal Trends of Concentration and Size Distribution of Ultrafine Particles Near Major Highways in Los Angeles, *Aerosol Sci. Technol.* 38:5–13.